Available online at www.ijapie.org

INTERNATIONAL JOURNAL OF ADVANCED PRODUCTION AND INDUSTRIAL ENGINEERING

IJAPIE-2018-04-226, Vol 3 (2), 25-37

IJAPIE
Connecting
Science & Technology
with Management.

A Journal for all
Products & Processes.

The Grain refinement of Aluminum alloys in Friction Stir Processing: A Review

N. Yuvaraj
(Department of Mechanical Engineering, Delhi Technological University, Delhi, India)
Email: yuvraj@dce.ac.in

Abstract : Most of the industrial applications based upon the surface properties. Aluminum and its alloys are mostly used in the surface application industries due to their excellent mechanical and corrosive properties. However, it exhibits in poor tribological properties. To enhance the mechanical and wear properties of the material grain refinement mechanism is to be incorporated. To improve the surface properties of the material the Friction stir Processing (FSP) Technique is mostly used nowadays. FSP plays an important role in modifying the surface in an efficient, environmentally friendly and economical manner. This review article describes the current status of the FSP Technology in grain refinement of Aluminum alloys.

Keywords: Friction Stir Processing, Aluminum, Grain size, Hardness, Wear

I. INTRODUCTION

In most of the engineering applications, aluminum alloys are widely used. Unfortunately, many of the aluminum alloys may be strong or ductile but rarely both at once. To retain the ductility and increase the strength of the material, grain refinement is to be incorporated [1]. FSP is used to produce fine grain, ultra-fine grain and refined nanocrystalline materials. It also eliminates inherent defects such as pores, oxide films and secondary particles in the base material and thereby improves its strength and ductility [2]. FSP creates uniform fine grain microstructure with significant grain boundary misorientation features, which are essential for enhancing the super plastic properties of the aluminum and its alloys.

FSP is a very effective route to improve the microstructure of cast aluminum alloys by (i) breaking up coarse silicon particles and disperse them into the matrix in a uniform manner. (ii) breaking up the coarse α-Al dendrites and refine the grain structure and (iii) eliminating the casting defects [3]. Friction Stir Processing (FSP) is a new surface modifying technique which is based on the principle of Friction Stir Welding (FSW). FSW was invented by The Welding Institute (TWI), UK in the year 1991 [4]. FSP is carried out by rotating and a plunging a specially designed hardened non-consumable tool with a shoulder and a small pin into a fixed work piece, and the tool is traversed along the line of interest. Friction between the shoulder and the work piece causes localized heating that softens and plasticizes the work material at the processing zone. The rotating pin generates intense plastic deformation due to the stirring action which results in fine and equiaxed grain structure which is called as stir zone. There is a narrow Thermo Mechanically Affected Zone (TMAZ), Heat Affected Zone (HAZ) and unaffected base material exists [5-7].

Table 1 The general terms used in FSP

Tool Shoulder	Part of the FSP tool which rotates and normally disc shaped and forms the processing region.
Tool Pin	The FSP tool pin extends from the shoulder and enters into the work piece.
Advancing side	The velocity vector of tool rotation and traverse direction are similar.
Retreating side	The velocity vector of tool rotation is opposite to traverse direction.
Plunge depth	The depth of the lowest point of the shoulder below the surface of the processed plate.
Tool rotational speed	The tool rotational speed is the number of revolutions per minute (rpm) of the tool about its axis.
Tool traverse speed	The tool traverse speed is the speed (mm/min) of the tool traverse through the processing line.

Fig. 1 shows the schematic drawing of friction stir processing. The general terms used in FSP is presented in Table 1. FSP is the most significant technique available for surface modification and it is a 'green' technology due to its energy efficient, environmentally friendly, an absence of fumes and versatility. The main advantages and limitations of the FSP are presented in Table 2. The list of attributes related to the FSP is shown in Fig. 2. The purpose of this article is to

review the current state of FSP technology in Aluminum based alloys.

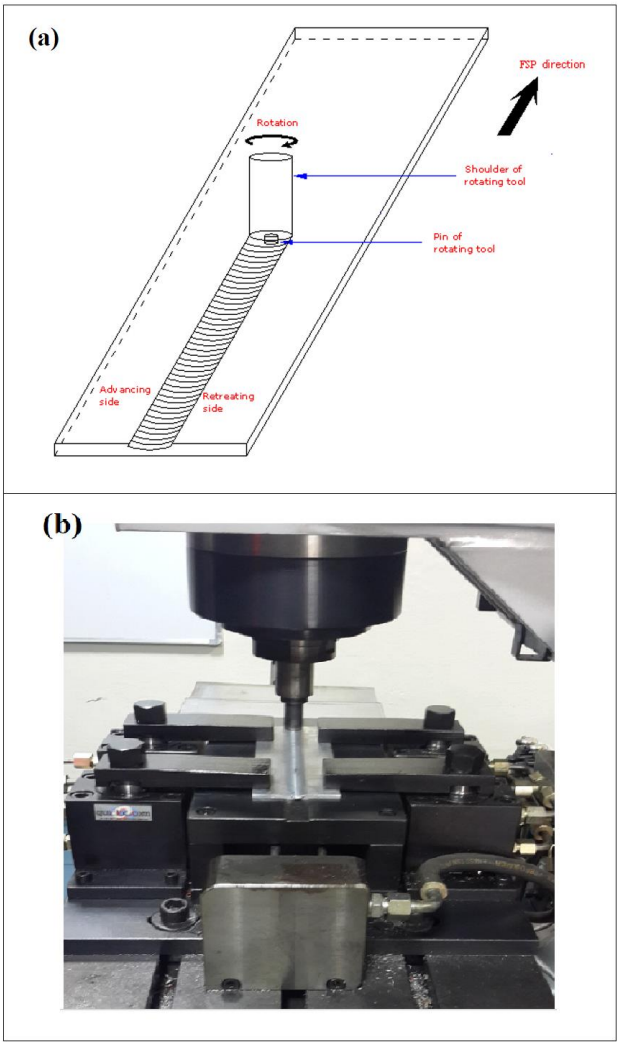

Fig. 1 Friction stir processing (a) schematic drawing (b) Experimental set up

II. GRAIN REFINEMENT

During FSP, materials are heavily deformed at the zone nearest to the pin tool, and there will be a large strain due to high temperature. The various mechanisms are responsible for refinement of grain size in the Stir Zone (SZ). The mechanisms are such as Dynamic Recovery (DRV), Continuous Dynamic Recrystallization (CDRX) and Discontinuous Dynamic Recrystallization (DDRX) [10-13]. FSP creates uniform fine grain microstructure with significant grain boundary misorientation features, which are important for enhancing the hardness and super plastic properties of the aluminum and its alloys. The tensile properties of the processed samples increase with decrease in grain size. As per Hall-Petch relationship [14].

$\sigma_s = \sigma_o + k_y d^{-1/2}$.... (1)

There σ_s and σ_o are constants; d is the average grain size. From this equation, σ_s is inversely proportional to grain size. According to this relationship decrease in grain size results in higher strength at stir zone.

Table 2 Benefits and limitations of FSP **[8]**

Benefits	
Technical	One-step processing technique No surface cleaning required Good dimensional stability and repeatability Facility of automation Depth of processed zone can be controlled by the pin length
Metallurgical	Solid state process Minimal distortion of parts No chemical effects and no cracking Grain refining and homogenization Excellent metallurgical properties Possibility to treat thermal sensitive materials
Energy	Low energy consumption since heat is generated by friction and plastic deformation Energy efficiency competing with fusion based processes as laser
Environmental	Green technique No fumes produced Reduced noise No solvents required for surface degreasing and cleaning
Limitations	New technique Lack of predictive models in FSP Keyhole at the end of each pass Need of a suitable fixture

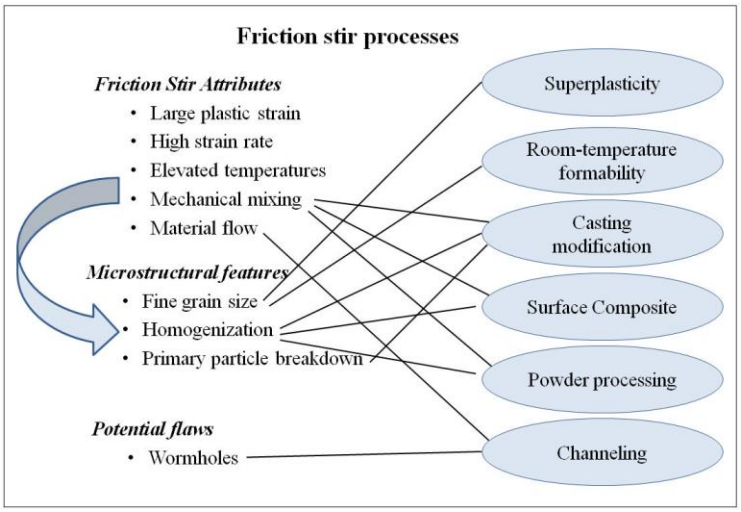

Fig. 2 Schematic view of list of attributes and links to the FSP process [9]

Several researchers have reported that the grain refinement of the aluminum alloys in the FSP takes place in the stir zone due to intense plastic deformation. The process parameters

are tool rotational speed, traverse speed, the number of passes, tool tilt angle, tool plunge depth, and the methods of cooling applied during FSP. Post heat treatment of the processed region also influences the microstructure [15-18]. Decrease in grain size of the material enhanced the mechanical properties such as hardness, strength, and ductility [19. The grain size of 0.7µm was obtained in Al-4Mg-1Zr samples subjected to FSP [20]. Ultra-fine grain sizes of < 1µm were obtained in under water FSP of Al2219-T6 alloys [21]. In the multipass submerged friction stir processing of Al 6061-T6 alloy the grain size is lesser than 200nm [22]. The grain size of 100nm to 400nm was observed in the processed Al 7075-T6 alloy [23].

Pradeep and Pancholi (2013) [24] friction stir processed on 5086 aluminum alloy with 50% overlap with different rotational speed and traverse speed combinations. The sample processed at tool rotational speed of 1024 rpm and traverse speed of 50mm/min the grain size was 12.6±3.1µm and the sample processed at tool rotational speed of 720 rpm and traverse speed of 155mm/min was 7.4±2.6µm. The base material grain size was 48±3.5µm. Lower heat input and high strain rates occur in the lower rotational speed and higher traverse speed specimens which resulted in smaller grains in the material with more ductile nature, and this process is suitable for obtaining the materials for super plastic forming. Cui et al., (2009) [25] were investigated the effect of different backing plate material & cooling methods on grain size of processed Al-Mg alloys. The different combination of backing plate and cooling methods were steel backing plate/air cooling, copper backing plate/air cooling and copper backing plate/water covered cooling. The average size of 2.7µm was obtained in the specimen of a copper backing plate with water covered cooling method, which is lower than other cooling method on processed samples. The average grain size of the processed specimens was decreased with lower rotational speed/traverse speed (ω/v) ratio. The less frictional heat is generated between the tool and workpiece which in turn causes reduction in grain growth in the stir zone.

El-Rayes and El-Danaf (2012) [26] have friction stir processed Al6082 alloy at tool rotational speed of 850 rpm and traverse speed of 90mm/min using a single pass. Second phase particles are homogeneously dispersed in the stir zone of the matrix with higher density. In the stir zone, severe plastic deformation and frictional heating result in the generation of fine-grained microstructure and the same is attributed to dynamic recrystallization. Sharifitabar, et al., (2011) [27] have reported that grain size of FSPed Al5052 alloy was decreases with increase in FSP passes.

The Fig. 3 shows the optical micrograph of stir zone of processed region of Al5052 alloy with with different number of FSP passes. Al-Fadhalah et al., (2014) [28] have studied the effect of number of passes on the grain size of friction stir processed Al 6063 alloy. Processed sample with two passes exhibited lower grain size in the stir region when compared to one pass processed samples. A post-Solution Heat Treated and Artificially aged (SHTA) two pass processed specimen had higher grain size (26-45µm) than the non SHTA two pass FSPed samples (2.9-4.0µm). It led to grain growth due to the formation of strengthening precipitates. The average grain size of the single pass friction stir processed Al2219 alloy was reduced to 6.2µm from the average grain size of the base material (67.4µm). Further increase in the number of passes to two and three has resulted in slight increase in average grain size value of 6.7µm and 7µm respectively. In multi passing, the heat input is slightly increased in the stir zone and reduces the size of intermetallic particles formed during solidification of aluminum alloy.

The formation of fine grain during FSP can be attributed to dynamic recrystallization [29]. Rao et al. (2014) have found that average silicon particle size of friction stir processed one pass and two passes of Al-30Si alloy are 2.5±1.8µm and 1.75±0.66µm respectively. The average silicon particle size in base material was 188± 20µm. The stirring action of the tool rotation breaks the coarse primary silicon particles and homogeneous distribution of silicon particles in the matrix. A similar type of results reported by Mahmoud (2013) [31] for friction stir processed cast aluminum alloy. Silicon particle size and aspect ratio of the processed alloy was decreased with increase in the number of FSP passes. The summary of some investigations on wrought and cast aluminum alloys using FSP are presented in Table 3 and Table 4 respectively.

The stir zone grain size, Tool materials and process parameters of some wrought and cast aluminum alloys processed by FSP are presented in Table 5 and Table 6 respectively.

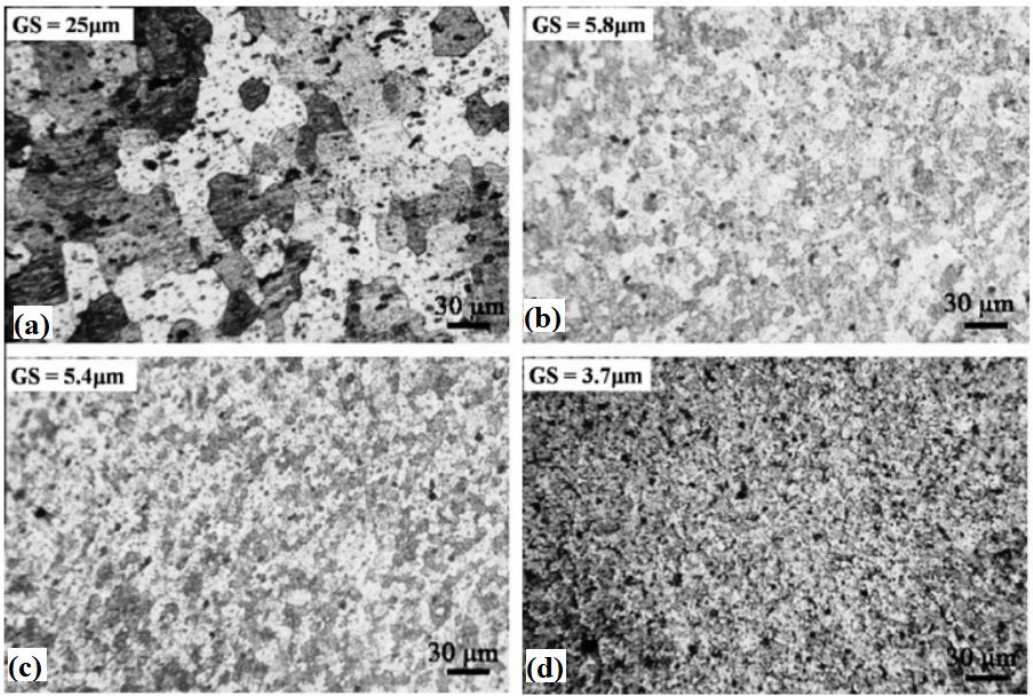

Fig.5. Optical micrograph of (a) Al5052 base alloy (b)FSPed stir zone one pass (b) FSPed stir zone two passes (c) FSPed stir zone four passes [27]

Table 3 Summary of the investigations on Wrought Aluminum Alloy using FSP

Material	Characteristic Studied	Prominent results	Reference
Al5083	Effect of cooling rate on the stir zone	Formation of ultra-fine grains and nano grains in the stir zone. The cooling effect may control the grain growth due to nuclei size and nucleation mechanisms.	[32]
Al5083	Deformation properties.	With tool rotational speed of 400rpm and traverse speed of 0.42mm/s highest super plastic elongation of 810% was obtained at 530^{o}C and 3x 10^{-2} s^{-1}.	[33]
Al 5083	Grain size	The grain size of FSPed was 6.1µm before rolling after rolling the grain size was increased to 10µm. The flow stresses were improved after rolling of the material.	[34]
Al5083	Hardness and wear behavior	Average hardness value of stir zone was increased to 93Hv and the base metal hardness was 88Hv. The lower friction coefficient (0.35) was observed in FSPed specimen and the base alloy friction coefficient was 0.62.	[35]
Al5083	Effect on rotational speed and post annealing effect	With increase in rotational speed grain size increases till 850 rpm after that there was no significant effect on grain size due to higher heat input. Post annealing treatment of the FSPed specimen eliminated the extra-large grains and formed more homogeneous grain structure.	[36]
Al5086-O	Mechanical properties.	The hardness was increased in FSP specimen due to the reduction of grain size. The grain size value of base metal was 48µm reduced to 4-6µm in FSPed specimen. Ductility values are better in all FSP processing conditions in comparison with base metal in both longitudinal and transverse directions.	[37]
Al5086-O	Super plastic behavior of multi pass (50% overlap) FSP	Ductility was uniform throughout the FSPed region in order to produce super plastic behavior. The material processed under low heat input (ω-1025 rpm v-50 mm/min) condition was more ductile than high heat input condition (ω-750 rpm v-155 mm/min).	[24]
Al1050	Texture development	The deformation took place in the alloy through rotating tool. The shear texture development occurred in the processed region due to tool induced in the stir zone.	[38]

Al1050	Hardness and tensile properties	Hardness and tensile strength of FSPed zone were increased 37% and 46% respectively.	[39]
Al1100	Electrical Conductivity	FSP of Al alloys lead to electrical conductivity changes of about 4% IACS (International Annealed Copper Standard). Processing Parameters of higher tool rotational speed versus tool travel speeds induce higher variations in the electrical conductivity and it is determinant for governing the electrical variation. Grain size was the major responsible factor for the electrical conductivity level and the electrical conductivity was decreased with decrease in grain size.	[40]
Al6061-T6	Ultra-fine grain size	Submerged FSP was an improved method to creation of ultra-fine-grained in bulk material. Grain size was reduced below than 200nm. The submerged water increases the cooling rate and slower the recrystallization kinetics and may yield bulk less size of grain size.	[22]
Al6061- T6	Effect on tool shoulder and natural aging.	Microstructural softening and hardness were greatly influenced by the frictional heating of the tool shoulder. Natural aging occurs more homogeneous in the the FSP region due to the stirring of tool pin.	[41]
Al6082-T651	Mechanical properties of multi pass FSP	Increase in number of passes in the stir zone the grain size increases and the ultimate tensile strength (UTS) of the material was decreases at a given traverse speed due to grain coarsening. Increase in traverse speed UTS of the specimen was increased.	[42]
Al6061	Bending Behavior	Bending behavior of FSPed plates were better than base material plates due to softened the plates in processed region and somewhat extended to the unprocessed region.	[43]
Al6063-T6	Process parameters and mechanical properties	Refined homogenized grain structure and enhanced mechanical was obtained by FSP at tool traverse speed of 40.2mm/min & rotational speed of 1200rpm &1400rpm with 10KN axial force. The processed region ultimate tensile strength, ductility and microhardness were increased to 46.5%, 133% and 33.4% respectively.	[44]
Al6063	Mechanical properties	Minimum grain size of 2.85µm was obtained in 50% overlapping FSPed specimen. Microhardness and tensile properties of post-heat treated FSPed samples shows higher than FSPed samples due to the formation of strengthening precipitates.	[45]
Al7075	Heat generation with different tool pins	Tool pin profile is an important parameter for heat generation during FSP. With the different tool pins i.e conical, square, pentagon and Hexagon, Pentagon tool pin generated maximum temperature due to larger effective pin area.	[46]
Al7075	Super plastic behavior	Multiple pass FSP enhanced the super plastic properties of material due to grain boundary sliding mechanism.	[47]
Al7075	Super plastic deformation behavior	FSP decreases the grain size of base material and enhances the super plastic behavior. During super plastic deformation dynamic grain growth and grain elongation were observed.	[48]
Al 7075	Super plastic behavior	Fine grain size of 6.2µm obtained through FSP due to strong pinning effect of second phase particles. FSPed specimen exhibited excellent superplastic behavior at 450-535^{o}C heating conditions.	[49]
Al2219-T87	Corrosion behavior	FSPed specimen exhibits the superior corrosion resistance when compared to the base material in all processing conditions. The immersion test, salt spray test and potentiodynamic test of multi pass sample were improved with comparison of one pass sample.	[29]
Al2219	Grain refinement	The microhardness of the underwater FSPed specimens decreased to 90-105Hv from base material hardness 123Hv even after the ultra-fine grain size of 1µm obtained at the stir zone, due to loss of metastable age-hardening precipitates and the formation of equilibrium precipitates.	[50]

Al2219-T6	Microhardness of water submerged FSP	Microhardness of water submerged FSPed specimen decreases to 95-105Hv, where base material hardness was 138Hv. The hardness was improved up to 140-150Hv by solutionizing and followed by water quenching & aging treatment of processed samples. Fine grains obtained by FSP were replaced by abnormally growth grains when subjected to post processing treatment due to loss of precipitate pinning during solutionizing.	[51]
Al2024-T4	Mechanical and tribological properties.	Maximum hardness (110Hv) was achieved in FSPed nugget zone due to fine equiaxed grain size of 4µm. The wear rate and friction coefficient reduced approximately 30%.	[52]

Table 4 Summary of the investigations on Cast Aluminum Alloy using FSP

Material	Characteristic Studied	Prominent results	Reference
Cast Al-Zn-Mg-Sc alloy	Tensile properties	FSP cast alloy with 1.8µm grain size material with solution heat treated and aging enhanced the yield strength(568MPa) upto 33% without change in ductility. The 5.5µm grain size material with solution heat treated and aging sample the yield strength was 303MPa with loss of ductility. The 0.68 µm grain size material with aging only the tensile strength was improved to 582MPa.	[53]
A356 cast alloy	Fatigue Properties	Fatigue crack initiation occurred in cast samples. Microstructural defects such as porosities, non metallic inclusions are main reasons lower fatigue life. In FSPed samples fine-grained structure resisting the fatigue crack initiation.	[54]
Cast Al-12Si	Mechanical and corrosive properties	The hardness and tensile strength of processed cast alloys were improved due to grain boundary strengthening mechanism and uniform dispersion of Si particles. The yield strength, ultimate tensile strength and elongation of FSPed cast alloy has increased from 63.10 to 65.03MPa, 138.42 to 159.39MPa and 2.65 to 9.87, respectively. The corrosion rate of the processed alloy was lower than base alloy	[55]
Cast Al-Si	Mechanical properties	Ultimate tensile strength of processed cast Al alloy was improved from 159 Mpa (base material) to 371 Mpa. The process parameters were rotational speed of 1400 rpm and transverse speed of 45mm/min.	[56]
Al-30Si	Corrosive Properties	The grain size(silicon particle) of the cast alloy decreased from 188µm to 2.1µm in one pass FSPed specimen processed at tool rotational speed of 350 rpm and traverse speed of 16mm/min . Further increase in number of passes to three the decrease in grain size (1.85µm) was not much significant. FSPed specimen with three passes specimen corrosion rate decreased in compare to one pass processed specimen and cast alloy. As per Hall-Petch relationship the corrosion rate and pitting potentional are inversely proportional to the grain size.	[57]
Al-30Si	Grain refinement	Average hardness of single pass FSP and two pass FSP Al alloy were lower than the base material due to dynamic recrystallization on softening of the grain boundary area. Silicon particle diameter is reducing from 188µm to 1.8µm in two pass FSP.	[58]
Al F357 (Al-7Si-0.6Mg)	Microstructure, and mechanical properties	FSPed samples eliminate porosity and uniform distribution of refined eutectic silicon particles in the processed zone. FSPed with T6 heat treat samples improves the tensile properties in compare with cast alloy.	[59]
Al 356	Processing parameters and microstructural refinement	High tool rotation or higher tool rotation/higher transverse speed ratios were responsible for homogenous distribution of fine silicon particles in the processed region. Silicon particle size at post FSP-T6 treatment sample was 0.83µm which was larger than FSP sample grain size of 0.42µm at the middle of the stir zone due to coarsen of silicon particles.	[60]
Al 356	Mechanical and Wear behavior	With increase in rotational speed the hardness of the stir zone was improved when compare with lower rotational speed due to uniform distribution of	[61]

		small and spherical Si particles throughout the FSP region. Wear resistance of the FSPed samples improved with increasing in rotational speed till 1000rpm, further there was no significant effect on wear behavior at higher rotational speeds.	
Al 356-T6	Mechanical behavior	With increase in rotational speed of FSPed specimen eliminates the casting porosity and effectively breaks the Si particles. Two pass FSP sample with rotational speed (1500rpm) & tool traverse speed (300mm/min) exhibited better tensile properties than one pass FSP sample. The YS, UTS and total elongation of two pass and one pass sample were 253Mpa, 305Mpa & 11% and 225Mpa, 278Mpa & 10% respectively.	[62]
Cast Al F357	Process parameters on grain growth	Single pass FSPed specimens showed the abnormal grain grown in the stir zone, whereas in the multi pass the grain size was decreased further and more resistant to abnormal grain growth.	[63]
Al 319	Mechanical properties	Enhanced microstructure and mechanical properties were observed in processed alloy when compared to base material. At 1200 rpm rotational speed with all feed rates better mechanical properties were observed.	[64]
Al 319 & Al 356	Mechanical properties	Casting porosity and dendritic microstructures were eliminated by FSP and more uniform microhardness was observed in the FSP region. Tensile properties were increased in the FSP region.	[65]
Cast Al 356	Wear and corrosive properties	Wear rate of cast alloy exhibited higher rate of 0.216µm/s and FSPed alloy exhibited lower wear rate of 0.0.14µm/s. The friction coefficient of the FSPed alloy was lower(0.15) than cast alloy (0.63). Corrosive resistance of the processed sample was improved due to higher cathodic reactivity of the surface and protects it from anodic attack.	[66]
Al 206 cast - T4	Mechanical properties	Ultimate tensile strength and ductility was increased in FSPed alloy and did not have much effect on heat treated FSPed alloy. Fatigue life of FSP specimens were increased due to elimination of casting porosity, size reduction of intermetallic particles. Heat treatment of FSPed specimens improved the fatigue properties marginally.	[67]
Al 2285 cast	Mechanical properties	In FSPed samples the yield and tensile strength improved around 30% and ductility increased to four-fold when compare with base alloy. FSPed samples with rotational speed of 1800rpm and feed rate of 12mm/min were obtained better mechanical properties.	[68]
Al 413 cast	Mechanical and wear properties.	The microstructural and mechanical properties of the cast alloy were improved through FSP with eliminating defects.	[69]

Table 5 Summary of the Tool materials, geometries and grain size of FSP of Al alloys

Material & Thickness (mm)	**Tool Material & Pin profile**	**Tool Geometry**	**Process parameters ω-rpm, v-mm/min**	**FSP condition**	**Grain size,**	**Reference**
Al5083	MP159 alloy Tapered cylindrical threaded pin	SD-24mm PD-6 mm PL-3mm	ω-400 & v-0.42mm/s	BM FSP	32.68µm 2.10µm	[41]
Al 5086-O 6mm	Hot die steel cylindrical pin	SD-24mm, PD-6 mm PL-3mm	ω-1025 & v-150	BM Single pass IMP[a] CMP[b]	48µm 2.9µm 5.5µm 4.5µm	[41]
Al 5086-O 6mm	Hot die steel Conical	SD-21mm, TD- 6mm, BD -4mm	ω-1025 & v -50 - sample-1 ω -720 & v -155 sample-2	BM Sample-1 Sample-2	48±3.5µm 12.6±3µm 7.4±2.6µm	[24]
Al5083 4mm	SKH-51 steel	SD- 15mm, PD-5.5mm, PL-3mm	ω - 450-1650 constant v – 33 1^{o} Tilt	BM ω -450 rpm FSP ω -650 rpm FSP	30-250µm 5.5µm 9.5µm	[36]

				ω-850 rpm FSP	12.8µm	
Al5083-H112	H13 tool Threaded pin	SD -18mm, PD-6mm, Tilt angle 3^{o}	ω-400 &v-200 Copper/steel backing plate,	Water/copper Air/steel Air/copper	2.7µm 8.5µm 5.0µm	[25]
Al 5083 ^{C}	MP159 alloy Conical threaded	SD-16mm TD-7mm, BD- 4.8mm	ω -400 & v-25.2	BM 0.49mn FSP 0.74mn FSP 1.00mn FSP	70µm 2.15±0.14µm 0.74±0.12µm 1.00±0.11µm	[70]
Al5083 5mm	H13 steel Threaded	SD-16mm PD-6 mm PL-3.2mm,	ω -750 & 1900, v - 25 4 passes 3^{o} Tilt	BM FSP ω-750 FSP ω-1900	60 µm 9.64µm 14.53µm	[71]
Al5083 6mm	Tungsten Carbide, Cylindrical	SD-11.5mm, PD-3mm, PL-3mm	ω - 710-1400 v-12.5-63 2^{o} Tilt	BM FSP	10µm 3µm	[72]
Al5052-H32 4mm	H13 steel	SD-13.6mm PD-5mm PL-3.7mm	ω-1600, v- 16 5^{o} Tilt	BM FSP-Two passes FSP-Four passes	25µm 5.4µm 3.7µm	[27]
Al 5052-H-112 10 mm	concaved	SD-20mm PD-6mm PL-3.2mm	ω-700-1700 & v-70 3^{o} Tilt	BM ω -700 rpm ω -1200 rpm ω-17000 rpm	82.24 µm 18.26µm 54.96µm 67.04µm	[73]
Al5052-H32	H13 steel Threaded pin	SD-18mm, PD-5mm, PL-5mm	ω-1200 & v-100, 4 passes	BM-Annealed BM-Wrought FSP- Annealed FSP Wrought	49.4µm 9.7µm 9.7µm 6.3µm	[74]
Al-Mg alloy-5mm	H13 steel Threaded pin	SD-18mm, PD-5mm, PL-5mm,	ω-1400 & v-50 2.5^{o} Tilt	BM FSP air cooling FSP water/dry ice FSP Liquid nitrogen cooling	49.4µm 9.9µm 1.8µm 1.0µm	[75]
Al5059 - 6.3 mm	---	SD-10mm& PD-4mm SD-12mm & PD-5mm	ω -1130 & v- 30 Counter clock wise ω - 454, v-30	BM 2 pass 3 pass	- 1-2µm 200-500nm	[76]
Pure Al 12mm	M2 steel	SD-12mm, PD-3mm, PL-2.1mm	ω - 640 & v 150	BM FSP	84µm 3µm	[77]
Al1100 5mm	1.2080 tool steel, Cylindrical	SD-18mm, PD-6mm, PL-4mm,	ω – 450-2000 & v – 10-100, plunge depth 0.2mm 3^{o} Tilt	BM ω – 560 & v -20 ω - 720 & v -10 ω - 720 & v -20 ω - 720 & v -30 ω - 900 & v -20	27µm 17±1.2µm 21±0.9µm 13±0.6µm 18±01.3µm 22±01.5µm	[78]
Al 1050	---	SD-12mm, PD-3mm PL-2.1mm	ω -1200 & v-50 3^{o} Tilt	FSP- One pass FSP-Two pass FSP-Three pass	15µm 10µm 18 µm	[79]
Al2219-T87-5mm	HSS Threaded Pin	PL- 2mm	ω - 1200 & v -22.2	BM 1 pass FSP 3 pass FSP	67.4µm 6.2µm 7.0µm	[28]
Al2219-T6 2.5mm	--	-	ω -1000 & v 200-400	BM Under water FSP	17µm 1.3µm	[50]
6061-T6 3.2 mm	Tool Steel	SD-19.1mm, PD-3.18mm,	ω -1000 & v -25-101.4	Base material Submerged FSP	50µm 100-200nm	[22]

		PL-2.79mm				
Al6082-T651 6mm	Mo-W tool steel concentric square pin	SD-15mm, EL-6mm, PL- 5mm	ω -850 & v -90	1 pass FSP 2 pass FSP 3 pass FSP	11.8µm 12µm 15µm	[42]
Al6082 10mm	HCHCr steel Threaded Pin	SD-18mm PD-6 mm PL-5.5 mm	ω -1200 & v - 60 Axial Force-10kN	Base material FSP	55µm 10µm	[80]
Al6063 12mm	H13 steel,	SD-14mm PD-4mm PL-4mm	ω - 600 & v - 145	BM FSP FSP-Heat treated	- 2.8-4.3µm 30.9-34.8µm	[27]
Al7075 6.4 mm	MP 159 alloy Steel Right hand screw	SD-25mm, PD-6.4mm, PL-6.4.	ω - 400 & v 50 3° Tilt	BM 1 pass FSP 2 pass FSP 3 pass FSP 4 pass FSP	-- 4.7±2.3µm 46±2.1µm 4.6±2.6µm 5.4±2.7µm	[47]
SD-Shoulder diameter, PD-Pin diameter, PL-Pin length, TD-Top diameter, BD-Bottom diameter, EL-Edge Length, (ω)-Tool rotational speed, rpm, (v)-Traverse speed mm/min, a-Intermittent multipass (IMP) b-Continuous multipass (CMP), c- with different mn contents						

Table 6 Summary of the Tool materials, geometries and mean Silicon particle size of FSP of cast Al alloys

Material & Thickness, mm	**Tool Material & Pin profile**	**Tool Geometry**	**Process parameters rpm ω-rpm, v-mm/min**	**FSP condition**	**Si particle size, µm (mean)**	**Ref**
A356 10mm	H-13, threaded pin	SD-20mm, PD-6mm, PL-3.7mm	ω -500-1250 & v-50 3° Tilt	BM FSP- ω -500 FSP- ω -1000 FSP- ω -1250	16.2 µm 8.2 µm 4.0 µm 3.3 µm	[61]
A356 10mm	M42 tool, threaded Concave/conical pin	SD- 24mm RD-8mmin TD-4 mm PL-6.8mm	ω -1500 & v-300 3° Tilt	BM 1 PASS 2 PASSES 4 PASSES 5 PASSES	12.91±6.79 µm 3.14±3.07 µm 2.89±2.71 µm 2.59±2.02 µm 2.97±2.60 µm	[62]
A413	H-13, Hemisphere end, R4 curved shape	SD-26mm, PD-10mm, PL-9mm,	Sample-1 ω -900 & v -63 Sample-2 ω -1400 & v -20	Sample-1 FSP Sample-2 FSP	2 µm 8 µm	[69]
Al-30Si - 12mm	H13	SD-25mm, PD-11.5mm, PL-10mm	ω -350 & v-16	Cast alloy 1 pass FSP 2 pass FSP 3 pass FSP	188±18 µm 2.10±0.55µm 1.90±0.5µm 1.85±0.6 µm	[29]
F357 Investment cast 3.3mm	Stepped spiral conical pin	--	ω -1600 & v-139.7	BM-cast FSP Cast+T6 FSP+T6	- 1.87±1.70µm 7.2±4.50µm 2.41±1.72µm	[59]
SD-Shoulder diameter, PD-Pin diameter, PL-Pin length, (ω)-Tool rotational speed, rpm , (v)-Traverse speed mm/min						

III.SUMMARY AND FUTURE OUTLOOK

In this review article current development in FSP of Aluminum alloy have been addressed. During FSP the grain refinement and the particle distribution are mainly affected by the FSP process parameters such as tool traverse speed, tool rotational speed, shoulder to pin diameter, FSP pass number, tool tilt angle, cooling method are greatly influenced. Grain refinement is greatly

influenced for enhancement of mechanical, wear and corrosive properties.

ACKNOWLEDGEMENT

The author is thankful to Prof. S. Aravindan, Professor, Department of Mechanical Engineering, Indian Institute of Technology, Delhi and Prof. Vipin, HOD & Professor, Department of Mechanical Engineering, Delhi Technological University, Delhi for their valuable guidance to execute the work.

IV. REFERENCES

[1] Thomas WM, Nicholas ED, Needham, JC, Murch J, Temple-smith P Dawes CJ (1991). Friction Stir Butt Welding, International Patent Application No. PCT/GB92/02203.

[2] Hatch J.E, *Aluminum Properties and Physical Metallurgy* (American Society for Metals, Metals Park, OH, USA, 1984).

[3] Gibson, BT, Lammlein, DH, Prater, TJ., Longhurst, WR, Cox, CD, Ballun, MC, Dharmaraj J, Cook GE, Strauss AM. (2014). Friction stir welding: Process, automation, and control. *Journal of Manufacturing Processes 16:56-73.*

[4] Mahmoud TS, Mohamed SS (2012). Improvement of microstructural, mechanical and tribological characteristics of A413 cast Al alloys using friction stir processing. *Materials Science and Engineering A 558: 502-509.*

[5] Yuvaraj N, Aravindan S, Vipin. (2017) Wear Characteristics of Al5083 surface Hybrid Nano-composites by Friction Stir Processing. Trans. Ind. Inst 70:1111-1129.

[6] Ma ZY, Mishra RS, (2005). Development of ultrafine-grained microstructure and low temperature (0.48 Tm) superplasticity in friction stir processed Al–Mg–Zr. Scripta Materialia 53:75-80.

[7] Nandan R, DebRoy T, Bhadeshia HKDH, (2008). Recent advances in friction-stir welding – Process weldment structure and properties. Progress in Materials Science, 53:980-1023.

[8] Cartigueyen S, Mahadevan, K. (2015). Role of Friction Stir Processing on Copper and Copper based Particle Reinforced Composites – A Review. Journal of Materials Science and Surface Engineering 2:133-145.

[9] Mishra RS, Murray, Mahoney W. Friction stir welding and processing–e Book, (ASM International, Metal Park, USA 2007).

[10] McNelley TR, Swaminathan S, Su JQ. (2008). Recrystallization mechanisms during friction stir welding/processing of aluminum alloys. Scripta Materialia, 58:349-354.

[11] Yazdipour A, Shafiei MA, Dehghani K. (2009). Modeling the microstructural evolution and effect of cooling rate on the nanograins formed during the friction stir processing of Al5083. Materials Science and Engineering A 527:192-197.

[12] Ihara K, Miura Y. (2004). Dynamic recrystallization in Al–Mg–Sc alloys. Materials Science and Engineering A 387–389:647–650.

[13] Yuvaraj N, Aravindan S, Vipin. (2017). Comparison studies on mechanical and wear behaviour of fabricated aluminium surface nano composites by fusion and solid-state processing. Surface & Coatings Technology, 309:309-319.

[14] Izadi H, Sandstrom R, Gerlich AP. (2014). Grain Growth Behavior and Hall–Petch Strengthening in Friction Stir Processed Al 5059. Metallurgical and Materials Transactions A, 45A:5635-5644.

[15] Cam G, Mistikoglu S. (2014). Recent Developments in Friction Stir Welding of Al-alloys. Journal of Materials Engineering and Performance, 23:1936-1953.

[16] Marie-Noelle, Avettand-Fenoel, Aude simar, (2016). A review about Friction Stir Welding of metal matrix composites. Materials Characterization 120:1–17.

[17] Weglowski MS. Friction stir processing-State of the art, (2018). Archives of civil and Mechanical Engineering 18:114-129.

[18] Padhy GK, Wu, CS, Gao S, (2018). Friction stir based welding and processing technologies processes, parameters, microstructures and applications: A review. Journal of Materials Science & Technology 34:1–38.

[19] Li SX, Cui GR. (2007). Dependence of strength, elongation, and toughness on grain size in metallic structural materials. Journal of applied physics, 101: 083525-6.

[20] Mishra RS. Ma ZY. (2005). Friction stir welding and processing. Materials Science and Engineering R 50:1-78.

[21] Feng X, Liua H, Babu SS. (2011). Effect of grain size refinement and precipitation reactions on strengthening in friction stir processed Al–Cu alloys. Scripta Materialia 65:1057-1060.

[22] Hofmann DC, Vecchio KS. (2005). Submerged friction stir processing (SFSP): An improved method for creating ultra-fine-grained bulk materials. Materials Science and Engineering A 402:234-241.

[23] Su JQ, Nelson TW. Sterling CJ. (2005). Microstructure evolution during FSW/FSP of high strength aluminum alloys. Materials Science and Engineering A 405:277-286.

[24] Pradeep S, Pancholi V. (2013). Effect of microstructural in homogeneity on superplastic

behaviour of multipass friction stir processed aluminum alloy. Materials Science and Engineering A 561:78-87.

[25] Cui G.R. Ma Z.Y. Li SX. (2009). The origin of non-uniform microstructure and its effects on the mechanical properties of a friction stir processed Al-Mg alloy. Acta Materialia, 57:5718-5729.

[26] El-Rayes MM. El-Danaf EA. (2012). The influence of multi-pass friction stir processing on the microstructural and mechanical properties of Aluminum Alloy 6082. Journal of Materials Processing Technology 212:1157-1168.

[27] Sharifitabar M, Sarani A, Khorshahian S, Shafiee Afarani M. (2011). Fabrication of 5052Al/Al2O3 nano ceramic particle reinforced composite via friction stir processing route, Materials and Design 32:4164–4172.

[28] Al-Fadhalah KJ, Almazrouee AI, Aloraier AS. (2014). Microstructure and mechanical properties of multi-pass friction stir processed aluminum alloy 6063. Materials and Design, 53:550–560.

[29] Surekha K, Murty BS, Rao KP. (2008). Microstructural characterization and corrosion behavior of multipass friction stir processed AA2219 aluminum alloy. Surface and Coatings Technology, 202:4057-4068.

[30] Rao AG, Katkar VA, Gunasekaran G, Deshmukh VP. Prabhu N, Kashyap BP. (2014). Effect of multipass friction stir processing on corrosion resistance of hypereutectic Al–30Si alloy. Corrosion Science, 83, 198-208.

[31] Mahmoud TS. (2013). Surface modification of A390 hypereutectic Al–Si cast alloys using friction stir processing. Surface and Coatings Technology 228:209-220.

[32] Yazdipour A, Shafiei MA, Dehghani K. (2009). Modeling the microstructural evolution and effect of cooling rate on the nanograins formed during the friction stir processing of Al5083. Materials Science and Engineering A 527:192-197.

[33] Garcıa-Bernal MA, Mishra RS, Vermac R. (2009). Hernandez-Silva D. High strain rate superplasticity in continuous cast Al–Mg alloys prepared via friction stir processing, Scripta Materialia 60:850–853.

[34] Johannes LB, Charit I, Mishra RS, Verma R. (2007). Enhanced superplasticity through friction stir processing in continuous cast AA5083 aluminum. Materials Science and Engineering A. 464:351–357.

[35] Behna RA, Besharati MK, Akbari M. (2012). Mechanical properties, Corrosive Resistance, and Microstructural Changes during Friction Stir Processing of 5083 Aluminum Rolled plates. Materials and Manufacturing Processes 27:636-640.

[36] Chun-Yi Lin, Truan-Sheng Lui, Li-Hui Chen. (2011). Evaluation of rotational speed and post annealing effect on the microstructural effect on the microstructural homogeneity of friction stir processed 5083 aluminum alloy. TMS, Friction stir welding and processing VI, 315-321.

[37] Ramesh KN, Pradeep S, Pancholi V. (2012). Multipass Friction-Stir Processing and its Effect on Mechanical Properties of Aluminum Alloy 5086. Metallurgical and Materials Transactions A. 43A:4311-4319.

[38] Khorrami MS, Kazeminezhad M, Miyashita Y. (2017). The Correlation of Stir Zone Texture Development with Base Metal Texture and Tool-Induced Deformation in Friction Stir Processing of Severely Deformed Aluminum. Metallurgical and Materials Transactions A 48A:188-197.

[39] Kwon YJ, Shigematsu I, Saito N. (2003). Mechanical properties of fine-grained aluminum alloy produced by friction stir process. Scripta Materialia 49:785-789.

[40] Santos TG, Miranda RM, Vilaca P, Teixeira JP. (2011). Modification of electrical conductivity by friction stir processing of aluminum alloys. International Journal of Advanced Manufacturing Technology 57:511-519.

[41] Woo W, Choo H, Brown DW, Feng Z. (2012). Influence of the Tool Pin and Shoulder on Microstructure and Natural Aging Kinetics in a Friction-Stir-Processed 6061–T6 Aluminum Alloy. Metallurgical And Materials Transactions A 38A:69-76.

[42] El-Rayes MM, El-Danaf EA. (2012). The influence of multi-pass friction stir processing on the microstructural and mechanical properties of Aluminum Alloy 6082. Journal of Materials Processing Technology 212:1157-1168.

[43] Miles MM, Mahoney MW, Fuller CB. (2006). Prediction of Bending Limits in Friction-Stir-Processed Thick Plate Aluminum. Metallurgical and Materials Transactions A. 37A:399-404.

[44] Karthikeyan L, Senthil Kumar VS. (2011). Relationship between process parameters and mechanical properties of friction stir processed AA6063-T6 aluminum alloy. Materials and Design. 32:3085-3091.

[45] Al-Fadhalah KJ, Almazrouee AI, Aloraier AS. (2014). Microstructure and mechanical properties of multi-pass friction stir processed aluminum alloy 6063. Materials and Design 53:550-560.

[46] Patel VV, Badheka VJ, Kumar A. (2017). Influence of Pin Profile on the Tool Plunge Stage

in Friction Stir Processing of Al–Zn–Mg–Cu Alloy. Trans Indian Inst Met 70:1151-1158.

[47] Johannes LB, Mishra RS. (2007). Multiple passes of friction stir processing for the creation of superplastic 7075 aluminum. Materials Science and Engineering A. 464:255-260.

[48] Ma ZY, Mishra RS, Mahoney MW. (2002). Superplastic deformation behavior of friction stir processed 7075Al alloy. Acta Materialia 50:4419-4430.

[49] Wang K, Liu FC, Xue P, Xiao BL, Ma ZY. (2015). Effects of heating rates on microstructure and superplastic behavior of friction stir processed 7075 aluminum alloy. J Mater Sci 50:1006-1015.

[50] Feng X, Liua H, Suresh Babu S. (2011). Effect of grain size refinement and precipitation reactions on strengthening in friction stir processed Al–Cu alloys, Scripta Materialia 65:1057-1060.

[51] Li HJ, Feng XL. (2013). Effect of post-processing heat treatment on microstructure and microhardness of water-submerged friction stir processed 2219-T6 aluminum alloy. Materials and Design 47:101-105.

[52] Zahmatkesh B, Enayati MH, Karimzadeh F. (2010). Tribological and microstructural evaluation of friction stir processed Al2024 alloy. Materials and Design. 31: 4891-4896.

[53] Charit I, Mishra RS. (2018). Effect of friction stir processed microstructure on tensile properties of an Al-Zn-Mg-Sc alloy upon subsequent aging heat treatment. Journal of Materials Science & Technology 34:214-218.

[54] Nelaturu P, Jana S, Mishra RS, Grant G, Carlson BE. (2018). Influence of friction stir processing on the room temperature fatigue cracking mechanisms of A356 aluminum alloy. Materials Science & Engineering A 716:165-178.

[55] Sun HH, Yang S, Jin D. (2017). Improvement of Microstructure, Mechanical Properties and Corrosion Resistance of Cast Al–12Si Alloy by Friction Stir Processing. Trans Indian Inst Met https://doi.org/10.1007/s12666-017-1232-5.

[56] Tsai FY, Kao PW. (2012). Improvement of mechanical properties of a cast Al–Si base alloy by friction stir processing. Materials Letters 80:40–42.

[57] Rao AG, Katkar VA, Gunasekaran G, Deshmukh VP, Prabhu N, Kashyap BP. (2014). Effect of multipass friction stir processing on corrosion resistance of hypereutectic Al–30Si alloy. Corrosion Science. 83: 198-208.

[58] Rao AG, Rao BRK, Deshmukh VP, Shah AK, Kashyap BP. (2009). Microstructural refinement of a cast hypereutectic Al–30Si alloy by friction stir processing. Materials Letters 63:2628-2630.

[59] Jana S, Mishra RS, Baumann JA, Grant G. (2010). Effect of Friction Stir Processing on Microstructure and Tensile Properties of an Investment Cast Al-7Si-0.6Mg Alloy, Metallurgical and Materials Transactions A 41A: 2010-2507.

[60] Ma ZY, Sharma SR Mishra RS. (2006). Effect of friction stir processing on the microstructure of cast A356 aluminum. Materials Science and Engineering A 433: 269-278.

[61] Alidokht SA,Abdollah-Zadeh A, Soleymani S, Saeid T, Assadi H. (2012). Evaluation of microstructure and wear behavior of friction stir processed cast aluminum alloy. Materials Characterization 63:90-97.

[62] Cui GR, Ni DR, Ma ZY, Li SX. (2014). Effects of Friction Stir Processing Parameters and In Situ Passes on Microstructure and Tensile Properties of Al-Si-Mg casting. Metallurgical and Materials Transactions A 45A:5318-5331.

[63] Jana S, Mishra RS, Baumann JA, Grant G. (2010). Effect of process parameters on abnormal grain growth during friction stir processing of a cast Al alloy. Materials Science Engineering A. 528:189-199.

[64] Karthikeyan L, Senthil Kumar VS, Padmanabhan KA. (2010). On the role of process variables in the friction stir processing of cast aluminum A319 alloy, Materials and Design 31:761–771.

[65] Santella ML. Engstrom T. Storjohann D, Pan DY. (2005). Effects of friction stir processing on mechanical properties of the cast aluminum alloys A319 and A356. Scripta Materialia 53:201-206.

[66] Madhusudhan Reddy G, Srinivasa Rao K. (2010). Enhancement of wear and corrosion resistance of cast A356 aluminium alloy using friction stir processing. Transactions of The Indian Institute of Metals 63:793- 798.

[67] Kapoor R, Kandasamy K, Mishra RS, Baumann JA, Grant G. (2013). Effect of friction stir processing on the tensile and fatigue behavior of a cast A206 alloy. Materials Science & Engineering A 561:159-166.

[68] Karthikeyan L, Senthilkumar VS, Balasubramanian V, Natarajan S. (2009). Mechanical property and microstructural changes during friction stir processing of cast aluminum 2285 alloy. Materials and Design 30:2237-2242.

[69] Mahmoud TS, Mohamed SS. (2012). Improvement of microstructural, mechanical and tribological characteristics of A413 cast Al alloys using friction stir processing. Materials Science & Engineering A 558: 502-509.

[70] Garcia-Bernal MA, Mishra RS, Verma R, Hernández-Silva D. (2012). Hot deformation behavior of friction-stir processed strip-cast 5083 aluminum alloys with different Mn contents. Materials Science and Engineering A, 534: 186-192.

[71] Zohoor M, Besharati Givi MK, Salam P. (2012). Effect of processing parameters on fabrication of Al–Mg/Cu composites via friction stir processing. Materials and Design 39:358–365.

[72] Abdi Behna R, Besharati MK, Akbari M. (2012). Mechanical properties, Corrosive Resistance, and Microstructural Changes during Friction Stir Processing of 5083 Aluminum Rolled plates. Materials and Manufacturing Processes 27:636-640.

[73] Yong-Ha Jeong, Md. Abu Mowazzem Hossain, Sung-Tae Hong, Kyung-Sik Han, Kwang-Jin Lee, Ju-Won Park, Heung Nam Han. (2015). Effects of Friction Stir Processing on the Thermal Conductivity of a Strain-Hardened Al-Mg Alloy. International Journal of Precision Engineering and Manufacturing 16:1969-1974.

[74] Khodabakhshi F, Simchi A, Nosko AKM, Vec PS. (2014). Strain Rate Sensitivity, Work Hardening, and Fracture Behavior of an Al-Mg TiO2 Nanocomposite Prepared by Friction Stir Processing, Metallurgical And Materials Transactions A 45A:4073-4088.

[75] Khodabakhshi F, Gerlich AP, Simchi A, Kokabi AH. (2015). Cryogenic friction-stir processing of ultra fine-grained Al-Mg-TiO2 nanocomposites, Materials Science & Engineering A 620:471–482.

[76] Izadi H, Gerlich AP. (2012). Distribution and stability of carbon nanotubes during multi-pass friction stir processing of carbon nanotube/aluminum composites. Carbon 50:4744-4749.

[77] Yadav D. Bauri R. (2012). Effect of friction stir processing on microstructure and mechanical properties of aluminium. Materials Science and Engineering A. 539:85–92.

[78] Mosallaee M, Dehghan M (2014). Improvement of Structural and Mechanical Properties of Al-1100 Alloy via Friction Stir Processing. Journal of Materials Engineering and Performance 23:3786-3793.

[79] Khorrami MS, Kazeminezhad M, Kokabi AH. (2014). The effect of SiC nanoparticles on the friction stir processing of severely deformed aluminium. Materials Science & Engineering A, 602:110-118.

[80] Thangarasu A, Murugan N. Dinaharan I. Vijay SJ. (2015). Synthesis and characterization of titanium carbide particulate reinforced AA6082 aluminium alloy composites via friction stir processing. Archives of Civil and Mechanical Engineering, 15:324-334.